2017

Towards a Prediction of Landscape Evolution from Chemical Weathering and Soil Production

Eric Alan Jackson
Wright State University

TOWARDS A PREDICTION OF LANDSCAPE EVOLUTION FROM CHEMICAL WEATHERING AND SOIL PRODUCTION

A thesis submitted in partial fulfillment of the requirements for the degree of Master of Science

By

ERIC ALAN JACKSON
B.S., Wright State University, 2013

2017
Wright State University

WRIGHT STATE UNIVERSITY

GRADUATE SCHOOL

December 15, 2017

I HEREBY RECOMMEND THAT THE THESIS PREPARED UNDER MY SUPERVISION BY Eric Alan Jackson ENTITLED Towards a Prediction of Landscape Evolution from Chemical Weathering and Soil Production BE ACCEPTED IN PARTIAL FULFLLMENT OF THE REQUIREMENTS FOR THE DEGREE OF Master of Science.

Allen Hunt, Ph.D.
Thesis Director

Jason Deibel, Ph.D.
Chair, Department of Physics

Committee on
Final Examination

_____
Thomas Skinner, Ph.D.

_____
Jerry Clark, Ph.D.

_____
Barry Milligan, Ph.D.
Interim Dean of the Graduate School

ABSTRACT

Jackson, Eric Alan. M.S. Department of Physics, Wright State University, 2017. Towards a Prediction of Landscape Evolution from Chemical Weathering and Soil Production.

The time evolution of a periodic landscape under the influence of chemical weathering and physical erosion is computed. The model used incorporates weathering and soil production as a flux limited reaction controlled by groundwater flow. Scaling of the flow rate is obtained from a percolation theoretic treatment. The erosion of the soil material produced by this process is modeled by the diffusion of elevation, as consistent with downslope soil transport proportional to the tangent of the angle of the topography, and application of the equation of continuity to surface soil transport. Three initial topographies are examined over a periods of thousands of years and resulting landforms and soil productivity compared. Differences in productivity between these cases are found to occur primarily within a short time span of hundreds of years. Times for propagation of a disturbance in one layer to another are also obtained.

TABLE OF CONTENTS

LIST OF FIGURES

LIST OF TABLES

1. Introduction

The evolution of the Earth's surface is a complex interplay of many processes. The formation, destruction, and movement of tectonic plates driven by energy from the Earth's core takes place under the influence of local variations in thermodynamic variables and can lead to a wide range of landforms. These in turn influence atmospheric patterns and create local climates affecting how the landscape is eroded. The liberation of sediment from bedrock and its transport can have profound consequences on the weight of a plate at a particular location, this may result in substantial contortion of the crust. In the Himalayas, for example, an extreme rise in the surface due to the collision of tectonic plates causes massive rainfall on one side of the range (and desert on the other). High precipitation in turn leads to significant erosion, removing mass from the region at a drastic rate. Because this lowers the weight atop an otherwise thick section of continental crust, the range as a whole remains buoyant and continues to rise. Taken together, this results in massive mountains and valleys, indeed the highest peaks in the world, see, for example Anderson [1]. The progress of this landscape evolution depends not only on how quickly sediment can be carried away, but also on the rates at which the solid bedrock can be rendered porous and mobile.

The purpose of this thesis is to develop a numeric solution of a weathering based landscape evolution model. This weathering will be considered as two processes; the

liberation of mobile soil grains from an underlying bedrock, and the redistribution of these grains across the surface by random forces. Together, these simulate the complex effect of chemical and physical action on the Earth's surface. The separation of weathering into two parts facilitates a partition of the landscape into two elevations; that of the soil and bedrock surface. The difference between them provides the soil depth and will be a primary quantity of interest.

The production of soil will be treated primarily as a chemical process in which dissolved reagents in groundwater react with bedrock to transform it into a porous material. Potentially, the reaction rate depends on a variety of factors including the particular compositions involved and the temperature of the environment. However, the flux of reagents to, or of reaction products away from, active reaction sites limits the rate at which weathering proceeds. Thus, the transport rate of solutes to the soil/bedrock boundary governs the soil production. An illustration of this process appears in figure 1. To determine the relevant solute transport times, a percolative model of porous media will be employed and a power-law dependent scaling in soil depth obtained. Percolation theory has a long history as a model of disordered media. A summary may be found in Stauffer and Aharony [2]. The range of applications is quite broad including solid-state physics, computer networks, and geology. In all of these fields, a primary consideration is the transport properties of a disordered system. Applied to geology, percolation can predict flow of groundwater and the influx of solutes to determine the rate at which new soil is produced from bedrock, as formulated by Hunt, et al [3]. The movement of the solute itself is also important. Carbon dioxide and its byproducts are prominent

reactants in the soil production process. This reaction may be the primary means by which the earth sequesters carbon from the atmosphere as has been suggested by Molnar and Cronin [4]. Accurate predictions of the rate at which this occurs then is critical for modeling climate change.

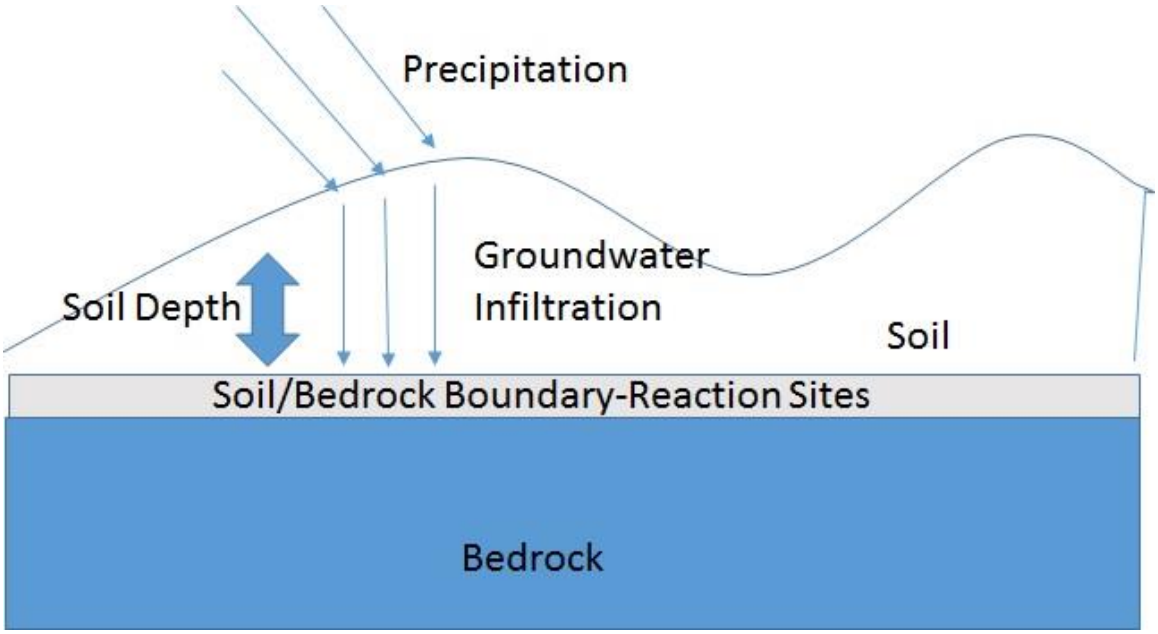

Fig. 1. Weathering model. Surface water with dissolved reagents penetrates the soil layer and eventually reaches the reaction sites at the bedrock boundary. The increase in soil depth changes future transport times and production rates.

The application of this soil production is complicated by the redistribution of the soil layer via erosion. This second process is treated as diffusive in nature. Diffusion has also been used extensively and is derived from the statistics of Brownian particles, so that both processes are based on fundamentally microscopic systems. Because the combination of the chemical weathering process and physical erosion allows for

changes in the elevation of both the upper and lower soil boundaries, a system of coupled partial differential equations will be necessary in the final formulation. The nature of the coupling, accounting for the scaling of transport times with depth, is non-linear and requires a numerical solution. The use of periodic boundary conditions was found to facilitate this computation. Results are presented for three variations of the initial conditions with consideration of the evolution of the landscape curvature, amount of soil produced, and comparisons with other models of the subject.

2. Theory

2.1 Erosion

The action of wind, rain, organisms, and other events on the Earth's surface results in erosion of the surface. A comprehensive model describing all of these is beyond the scope of this work. Instead, a simple model often used for the transport of heat, solutes, and many other quantities is employed. The net effect of many random events typically converges to a Gaussian distribution by the central limit theorem (CLT) [5]. Although the original statement of the CLT applies only to events with identical, independent distributions, extensions have since been made which show convergence even for sums of disparate distributions. The primary obstacle to applicability is strong correlations between events. In the absence of a more detailed description of the physical processes under consideration, this work will assume that convergence applies, at least approximately.

The random walk is a common treatment of the motion of particles acted upon by stochastic forces. A great deal of literature has been published on this subject. A basic treatment can be found in Reif [6]. In this model, a particle begins at some site on a discrete lattice and, at each time step, moves to an adjacent site probabilistically. The particular case of a regular two-dimensional lattice with the particle starting at the origin and with no directional bias is an often used example. There are a number of well-

known properties of this formulation. Because the process is symmetric, the average position of the particle remains the origin; an excursion in one direction is equally as likely as in the opposite and so the mean is 0. The magnitude of these excursions increases as the square root of the number of steps. When taken to the limit of infinitesimal steps, the result is a continuous-time random walk. In such a limit, the CLT applies and the distribution of positions takes a Gaussian form. Further, a Gaussian distribution (of zero variance), is the Dirac delta function, which is also the Green's function of the diffusion, or heat, equation, and can represent an initial point source. This allows the spreading of a collection of particles to be described by the diffusion equation:

$$\frac{\partial \rho}{\partial t} = D\nabla^2 \rho, \tag{1}$$

where ρ would represent a probability of finding the particle in a region of space for a single particle; but is interpreted as a concentration if many particles are considered. D is the "diffusion constant" governing the rate at which motion occurs for this continuous process. In keeping with the stipulation that each direction of the walk is equally weighted, D in this case is a scalar. Though the diffusion constant sets a typical speed of the diffusion process, a potentially significant technical problem is that solutions allow non-zero probabilities of finding a particle at arbitrary distances for all $t \neq 0$. Infinite propagation speeds are clearly non-physical, but generally pose no practical concern unless the behavior at very short times is relevant.

As mentioned above, diffusion has been used to model solute transport. However, in the case of macroscopic flow of the solvent, the sub-linear growth of displacement with time means the flow rate often dominates any such diffusive motion [7]. For this reason, the diffusion equation will be used for the erosion of soil particles, but the flow of solute requires a description of how water moves through the soil. Also, because random walk steps are uncorrelated, the process has no memory and cannot account for momentum. For the purposes of this work, this limitation precludes consideration of macroscopic flows of soil.

2.2 Flow in Porous Media

Porous media may be in the form of a connected object with holes, such as pumice, or a collection of small particles packed together. Soil is an example of the latter. It is a "grain supported medium" where these small particles (grains) rest upon one another under the influence of gravity, so they are connected despite not constituting a single, chemically bonded object. The size and shape of these grains vary widely as do the gaps between them. The simplest is the soil's porosity, ϕ, which is the volume fraction of empty space within the medium. Porosity describes how much empty/solid space there is, but not the structural arrangement of them. Information of how these spaces are partitioned into individual grain and pore and pore clusters is contained in the particle and pore size distributions. For a truly random medium, these functions, detailing the number of grains/pores of a given size, give a complete statistical description of the material. This is not the case when there are correlations in the spatial distribution of clusters or anisotropy in their orientations. These correlations contain additional

information about the medium and there may deviation from properties of uncorrelated media. Despite this, both pore and particle distributions are commonly thought to scale according to similar power laws compatible with percolation treatments and fractal models presented below. An important condition for this compatibility is that the medium be, in the mean, scale invariant, a common, but not universal observation [3]. Scale invariance is a key property of fractal models, they exhibit similar features across a range of length scales.

Transport depends on properties of both fluid and pore space. Both of these require some assumptions for tractability. For the fluid, incompressible, laminar flow will be assumed. Water is nearly incompressible unless very high pressures are involved. The effect of turbulence is often determined through the Reynolds number, Re. This quantity depends on flow rate, u; and the length of the flow space, l.

$$Re = \frac{\mathrm{u\,l}}{\mathrm{v}} \tag{2}$$

The quantity v is the kinematic viscosity of the fluid, on the order of $10^{-6}\ m^2/s$ for water at standard temperature. For a typical pore scale of 10^{-4} meters and flow rates of 10^{-6} m/s [8, 9], the Reynold's number is well below the ≈2000 range where flow becomes turbulent in a cylinder.

Under these conditions, Poiseuille's Law gives the flow through a cylindrical pipe:

$$\Delta p = \frac{8\mu l q}{\pi r^4}, \tag{3}$$

with p the pressure difference across the pipe; μ, the dynamic viscosity; and q the flow through it in units of m^3/s. In the soil, l is the length of the pore, and r is its radius. This form can be inverted to obtain an expression of the conductance, g, proportional to r^4/l. If it is assumed that the radius and length of a pore are equivalent in the pore statistics, as they should be in an isotropic, scale-invariant, medium, then this simplifies to a cubic dependence on radius of the conductance.

$$g \propto r^3 \tag{4}$$

This cylindrical flow can be employed if the pore space can be meaningfully partitioned into regions of appropriate geometry. In the capillary bundle model, often used by geologists, it is assumed that flow paths consist of cylindrical tubes of various radii. As this is equivalent to all pores aligned in series, the equivalent hydraulic conductivity is simply a summation over the distribution of radii multiplied by the dependence of conductance on radius. This clearly does not account for the complicated geometry and connectivity of the pore space, but results in reasonable approximations for certain types of soils [10].

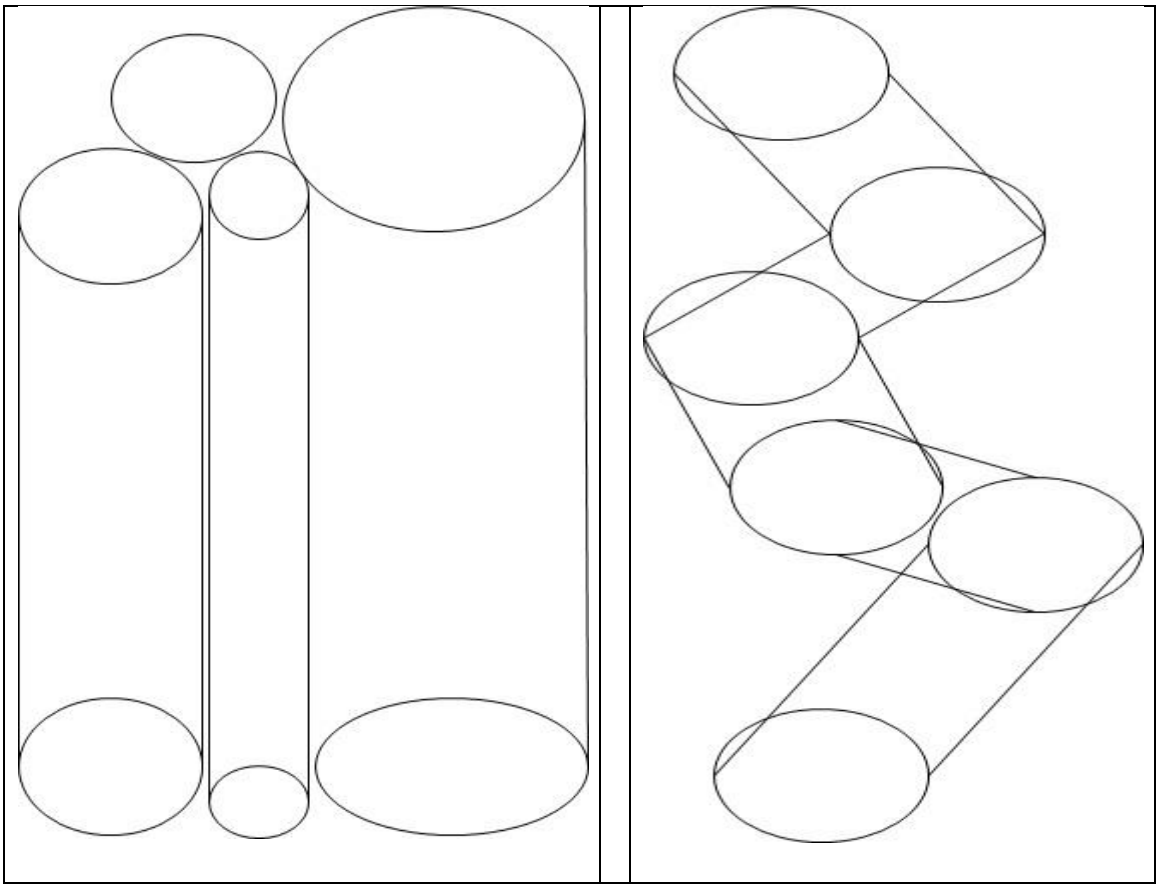

Fig. 2 Illustration of capillary tube model and tortuosity. Left, a bundle of cylinders of varying size as used in the capillary approximation. Right, tortuous flow path that must be accounted for as a correction to the simple model.

As a partial correction, a factor known as tortuosity can be introduced. This accounts for the path length while maintaining the tubular approximation. Several definitions of tortuosity exist [11], but here it will be taken as the ratio of the flow path length to the Euclidean distance traversed. It is often applied merely as an adjustable parameter as the capillary bundle lacks a basis for its prediction. While figure 2 provides an idea of the zig-zag pattern a path might take, it is more difficult to visualize how this scales with distance. Fractal models encapsulate the branching qualities expected of a real network

and predict a non-linear scaling rather simply a percent increase in path length. The appropriate fractal dimension for this has been obtained from percolation models.

2.3 Percolation Theory

Percolation theory refers to various models of connectedness in random media. The following discussion is based primarily on results presented in Stauffer and Aharony [2] and Hughes [12]. The simplest case may be that of a one-dimensional chain. This chain consists of a series of points, or sites, on a one-dimensional lattice. A site may be "occupied" or not. A number of occupied adjacent sites is referred to as an occupied cluster. If the probability of any one site being occupied is p, then the probability that a single cluster spans a lattice of size n, that it "percolates", is p^n. Clearly, as n goes to infinity, percolation only occurs at p=1. This result is trivial, but demonstrates an important property of percolation networks: the existence of an infinite connected cluster has a sharp cutoff in p at p_c, the "critical" probability or percolation threshold.

Higher dimensional lattices yield more interesting results. They also introduce additional parameters. The geometry of the lattice affects the number of neighboring points and thus, p_c. For example, each site of the square lattice has four neighbors and a threshold of approximately .59 while the triangle lattice has 6 neighbors and $p_c = 1/2$. The occupied network on these lattices has as its complement all clusters of unoccupied sites. For the square lattice only one of these can percolate at a time since $1 - p_c < p_c$. Except for a region of infinitesimal size, this also holds for the triangle lattice. It can be shown that if a percolating cluster of a certain type exists, there can only be one such

cluster. Thus, the existence of one infinite cluster precludes the existence of any other. This is not necessarily true in three dimensions where thresholds are much lower and this permits fluid flow through soil despite the necessary adjacency of particles in a grain supported medium.

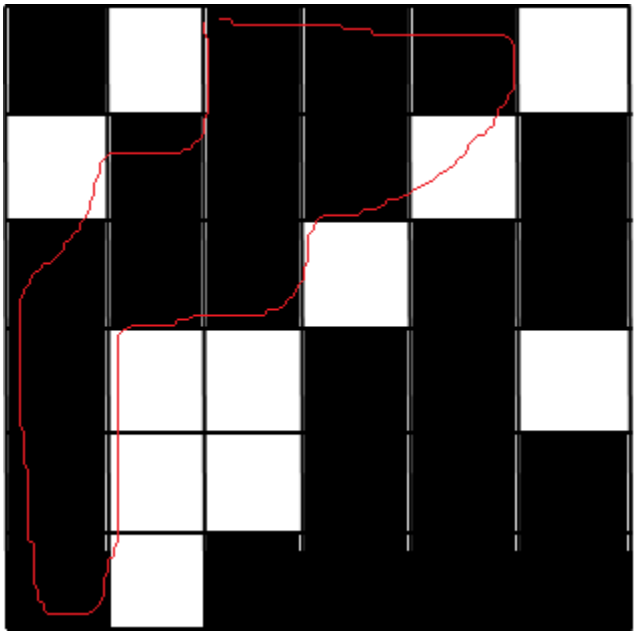

Fig. 3. Site percolation with p=.6 on a square lattice. The cluster circled in red spans the lattice.

The statistics of percolation strictly hold in the limit of an infinite lattice. A square lattice just above threshold is depicted above. For such a small lattice, the presence of a spanning cluster is not guaranteed. As the lattice grows, an occupation probability greater than p_c predicts the existence of such a cluster more and more accurately. The event that a percolating cluster exists is an example of a phase transition and occurs in a wide range of models in statistical physics. Quantities in these systems depend on an order parameter, in this case occupation probability, and its deviation from the critical value. A particularly important quantity is the correlation length.

$$\xi \propto (p - p_c)^{-\nu} \quad (5)$$

which describes the length of the largest finite cluster. The exponent, ν, is an example of a critical exponent. These define the scaling relationships common to models exhibiting critical phenomena. Across such models, it is found that their values are often the same and thus describe the behavior of many disparate systems, a property known as universality. The equivalent models make up a universality class; each class is largely determined by the dimensionality of the system rather than their microscopic geometries or the source of the physical interactions they simulate. The universality of percolation results provides a rationale for applying them to real systems for which the exact structure may not be known such as the pore space of soils.

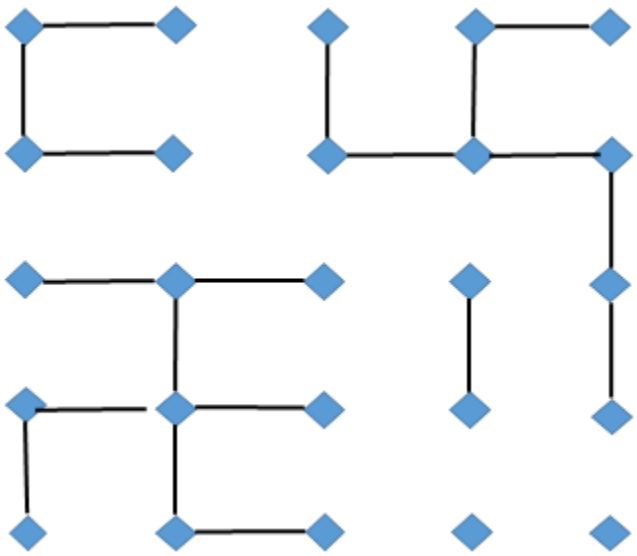

Fig. 4. Bond percolation with p=.4 on a square lattice. There is no spanning cluster in this example.

The percolation problems discussed above have addressed what is known as “site” percolation where the adjacency of occupied lattice points defines the network. There is also the “bond” percolation model where line segments between lattice points control

connectedness. These bonds may be open or closed analogously to the occupation or lack thereof of sites in the site model. An example for the square lattice is depicted in Figure 4. This lattice has a different threshold value than the site problem on the same geometry, but is equivalent to a different site problem. In fact, any given bond problem is equivalent to a, possibly unknown, site problem. The reverse is not true, the site formulation is known to be more general [13].

Despite this equivalence, more is known about the bond problem for some lattices and it may be more easily extended to models of conductivity. This will be useful for application to solute transport times. Suppose that each bond is associated with a conductance. For the binary, open/closed, cased, this is simply 0 or 1. Broader distributions with arrays of conductance values may be used. To determine the effective conductivity of such a network, the method of critical path analysis (CPA) will be used.

2.4 Critical Path Analysis

The premise of CPA, as developed by Ambegaokar et al [14] and others, is that because flow occurs preferentially on the fastest routes, a network above threshold can be pared down to include only links at or above a minimum conductivity necessary to span the lattice. Thus, this subset of the network is precisely at the percolation threshold. Though this identifies the controlling conductance, it does not necessarily define the optimal path as there may be additional connections “shorting” the critical path and increasing its conductivity. There is also some ambiguity in how to sum this reduced conductance

distribution due to the divergence of the length scale in a network at threshold, i.e. the correlation length, ξ, is infinite.

An argument due to Sheppard et al. [15] maintains that despite these complications, conductivity should scale with lattice size in a consistent manner. Numerical simulations of solute arrival times by Lee [16], using a "particle launching algorithm", suggest that this scaling with lattice size depends on the fractal dimensionality of the percolation backbone:

$$t \propto x^{D_b} \tag{6}$$

To obtain a rate from this relationship, it must be inverted and differentiated:

$$\frac{dx}{dt} \propto x^{1-D_b}, \tag{7}$$

where D_b is the backbone dimensionality. The backbone is the part of the percolating cluster not including dead ends which do not contribute to conductance. For the landscape model, the extent of the lattice, x, becomes the soil depth, f-g, the difference between the upper and lower soil boundaries. The z-axis elevations of these boundaries are denoted by functions f(x,t) and g(x,t) respectively. With this replacement, the scaling of production rates becomes:

$$\frac{dx}{dt} \propto (f-g)^{1-D_b} \tag{8}$$

The value of 1.87 for the backbone of a three-dimensional, random continuum percolation will be used in this work [15]. As the name suggests, these extend percolation to a continuous space rather than a discrete lattice. This extension makes

them an appropriate choice for use with other continuum models such as the diffusion discussed earlier. It also allows for application to pore space models described by continuous rather than discrete distribution functions, which is common.

The value of D_b is chosen for saturated conditions where the accessible pore space is completely filled by one type of fluid. When multiple fluids are present, such as water and air, D_b may differ depending on which fluid is displacing the other. However, evidence suggests that soil formation occurs only under wetting conditions (when water is advancing) and the value for D_b of 1.861 differs little from that of full saturation [17].

2.5 Combined soil production and erosion. Landscape evolution.

The shape of the landform over time has two contributions in this work. One is the conversion of bedrock into soil and the other the movement of this soil across the surface. While these two processes can both be thought of as erosion, they have been divided here for tractability. Erosion, as this thesis will refer to it, is prescribed by diffusion. Soil production is accounted for by the solute transport relationship from the previous section. Combining the rates from both processes yields the following system of equations:

$$\frac{\partial f}{\partial t} = D\frac{\partial^2 f}{\partial x^2} + \sigma\left(\frac{\rho_s}{\rho_r} - 1\right)\left(\frac{f-g}{x_0}\right)^{1-D_b} \tag{9a}$$

$$\frac{\partial g}{\partial t} = -\rho_r \sigma\left(\frac{f-g}{x_0}\right)^{1-D_b} \tag{9b}$$

Here ρ_s and ρ_r have been introduced to account for the differing densities of rock and soil. The soil density is the bedrock density divided by the volume fraction of the soil

corresponding to particles in a continuum model, and x_0 is a typical pore size and provides a natural length scale. The rate coefficients, D and σ, are typical soil erosion and groundwater infiltration rates, respectively. These values are taken from field data as the theoretical values are not universal.

A note must be made about the presence of boundaries. Percolation values are only exact for an infinite lattice. No physical system can meet such a requirement, but may approximate it quite closely. There is deviation from fractal behavior where the lattice does not extend to the correlation length and some local variance in flow rates are to be expected there. Thus, where the soil is shallow, there may be deviation from the predictions of percolation theory.

Equations 9a and b have no analytic solution of which the author is aware. Thus, a numerical simulation will be carried out.

3. Computation

All computational work is carried out in the Mathematica software package. As previously discussed, the "standard" diffusion equation has well-known analytic solutions. One method for approximating the present problem might be to make use of an analytic solution over some short time span, add to it the source term, and repeat. The analytic solver included in this package seemed capable of this, but only for a few iterations.

Instead, the numerical NDSolve algorithm was chosen utilizing some of the more advanced options outlined in online documentation provided by the software publisher [18]. This algorithm dynamically chooses mesh settings for its finite element analysis. However, the default options are poorly suited to solving this particular system. A pseudo-spectral difference order was chosen to maximize precision. A pseudo-spectral expands the solution as a truncated series of basis functions which must be evaluated at various times. This is accomplished by a Fourier transform which saves computation time. Because the Fourier transform works with periodic functions, this method performs poorly near discontinuities. The choice of periodic boundary conditions was made to avoid this issue. These must be explicitly specified to the solver. Periodic initial conditions alone are not sufficient. These conditions also allowed some generality in

specifying the problem. Mass of rock and soil is conserved without having to define arbitrary rates in and out of the system. This choice also approximates the infinite lattice on which the percolation results depend. The z-axis boundaries, of course, do not meet this criteria.

The shape of the initial boundary was chosen to be sinusoidal due to its simplicity, smoothness, and periodicity. The software is capable of interpolating a range of functions as periodic, but the use of non-periodic curves, such as a parabolic surface, led to high frequency oscillations in the solution, a known problem with pseudo-spectral methods. For this reason, computations involving other types of initial conditions were not considered for further analysis.

4. Results

4.1 Comparison of Initial Geometries

Results from three variations of initial conditions are compared. A sinusoidal surface layer atop flat bedrock (SvF), flat surface above curved bedrock (FvS), and both layers curved (SvS). A flat on flat geometry remains flat and does not exhibit interesting behavior. Although the model is fundamentally three-dimensional, only topographies with constant cross-sections along the y-axis are presented. Features in all dimensions were simulated, but analysis of their evolution will require further study. Whether the solution of these contains additional features of note requires further exploration of the parameters. A sample geometry is given in figure 5 while figure 6 illustrates the setup of the how solutions of the two layers will be presented.

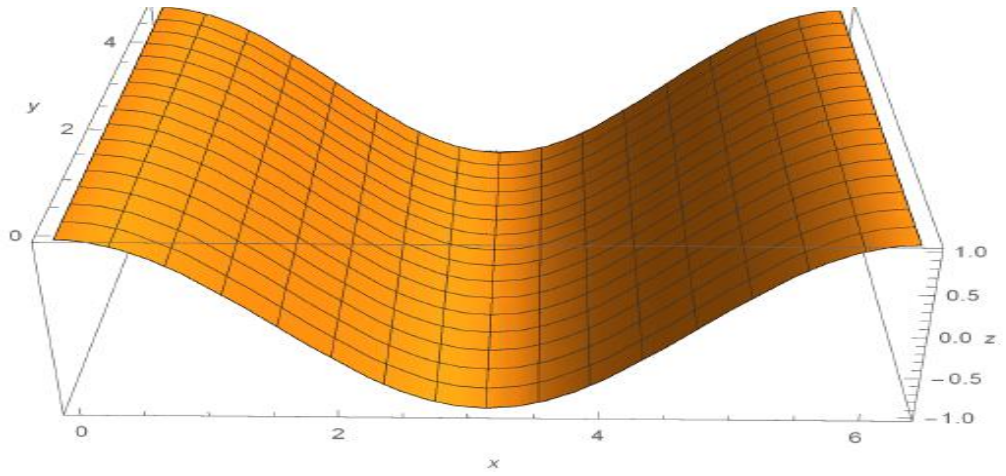

Fig. 5. Example of constant, sinusoidal hill cross section in the xz plane.

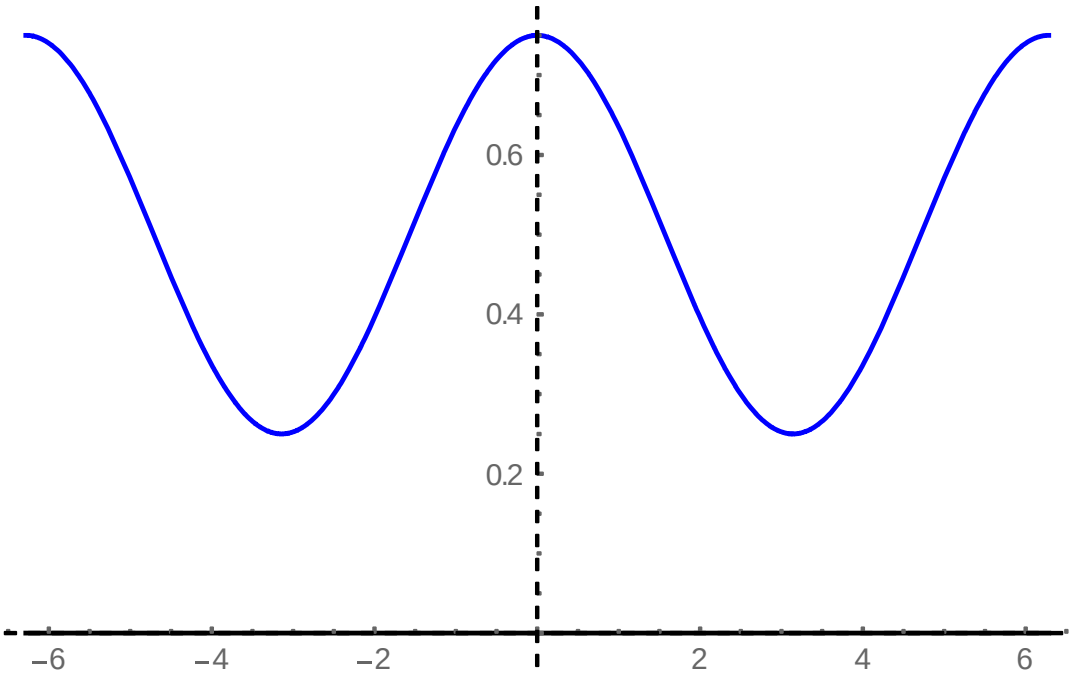

Fig. 6. Example (blue) soil surface and (black) bedrock boundaries.

For these calculations of equations 9a and 9b, D has been chosen as 50 cm^2/yr, the infiltration rate σ is taken to be .3 m/yr, x_0 is 30 microns, and soil with a porosity of 40% is used, resulting in a ratio of soil to rock density of 3/5. These values are somewhat typical of real environments [19]. The initial boundary conditions consist of straight line and/or sinusoidal functions with initial amplitudes of .25 meters with the upper and lower layers separated on average by half a meter.

The appropriate time scale over which to observe the solutions is somewhat arbitrary. Geologic scales may be many millions of years, but the use of periodic conditions precludes the removal of soil from the system and results in larger build-ups than would be expected in a real system as flow of soil away from the region is prohibited. The

morphology at very long times is also uninteresting as it converges to two flat layers asymptotically. Fortunately, a qualitative change in the system is observed at finite times. Consider the SvF case, a wave-like pattern can be discerned in the propagation of surface morphology to the bedrock. The curvature of the bottom approaches that of the initial surface layer and reaches a maximum amplitude before resuming asymptotic behavior. The same effect can be seen in the reverse, FvS, arrangement. Thus, a surface disturbance has a certain time over it which it alters the rock below and vice versa. This provides a characteristic time, t_c, over which to examine the evolution of the system. No clear time was found for the SvS system. Due to approximation in calculating the derivatives, these times may be somewhat imprecise. Although neither layer is truly sinusoidal past t_0, the separation of the highest and lowest point on a layer was taken as a good approximation of (twice) the amplitude and the change between subsequent differences compared. The times obtained, soil produced up to that time, and approximate surface and bedrock amplitudes at that time, can be found for each geometry in table 1a. Soil produced up to a given time is defined as:

$$\frac{\int((f(x,t)-g(x,t))dx-\int(f(x,0)-g(x,0))dx}{T}, \quad (10)$$

with T the period, 2π.

Characteristic time and values at that time	$\approx t_c(years)$	Soil Produced (meters)	Top Amplitude	Bottom Amplitude
Sine on Flat	800	.080	.005	.005
Flat on Sine	500	.056	.007	.235

Table 1a

In order to compare these cases with the SvS initial conditions, values at a fixed (and arbitrary) time are also given in Table 1b. The span of one thousand years appears to cover most of the interesting behavior, and differences in soil produced are largely attributable to the first few hundred years. Though bedrock curvature is longer lasting than that of the surface, and continues to produce more soil over long spans of time, it is this resistance to erosion even over relatively short time periods that accounts for most of the difference in soil production. Notice how the maximum amplitudes attained at characteristic times for the initially flat boundary are a small fraction of the initial curvatures. Indeed, in both cases it is less than the curvature decay in the other layer.

Values at 1000 yr	Avg. Soil Produced	Top Amplitude	Bottom Amplitude
Sine on Flat	.099	.002	.005
Flat on Sine	.105	.003	.225
Sine on Sine	.103	.005	.230

Table 1b

At t_c, the SvF case has very nearly become two sinusoids of the same amplitude, however this amplitude is small enough to be considered as flat. The FvS geometry potentially shows a more interesting intermediate phase, but seeing this requires an initial separation small enough to cause computational problems. The general behavior appears to be in line with the results in Ahnert [20] that bedrock shape dominates so long as erosion is not exceedingly large. Taking this into account and manipulating the initial amplitudes and separations, the pattern that emerges is that soil production rates are more strongly correlated with the average separation of the bedrock and surface layers than to the curvature of either.

The Sine on flat and sine on sine conditions for the same average separation produce almost exactly the same amount of soil over this time period. The surface of the double sinusoid flattens more rapidly than the soil/rock interface, but there are still clear in morphologies between the two cases. The reverse with a flat surface atop a sinusoidal interface produces soil far less quickly, apparently due to the variance in the surface layer, and therefore depth, eroding quickly relative to the influence of the lower layer.

The plots of figure 7 illustrate the short time span over which most significant behavior occurs. In 7a and 7b the flat surfaces reach their maximum curvature over this time and for 7c, the initially similar surface and bedrock have nearly converged to the FvS initial state.

The same conditions are plotted in figure 8 over a longer time-span and demonstrate the long-term asymptotic behavior expected of a diffusive model in the surface layer.

The latter two plots show that the bedrock retains its shape over long spans of time. The significant soil accumulation is likely unrealistic and attributable to the boundary conditions.

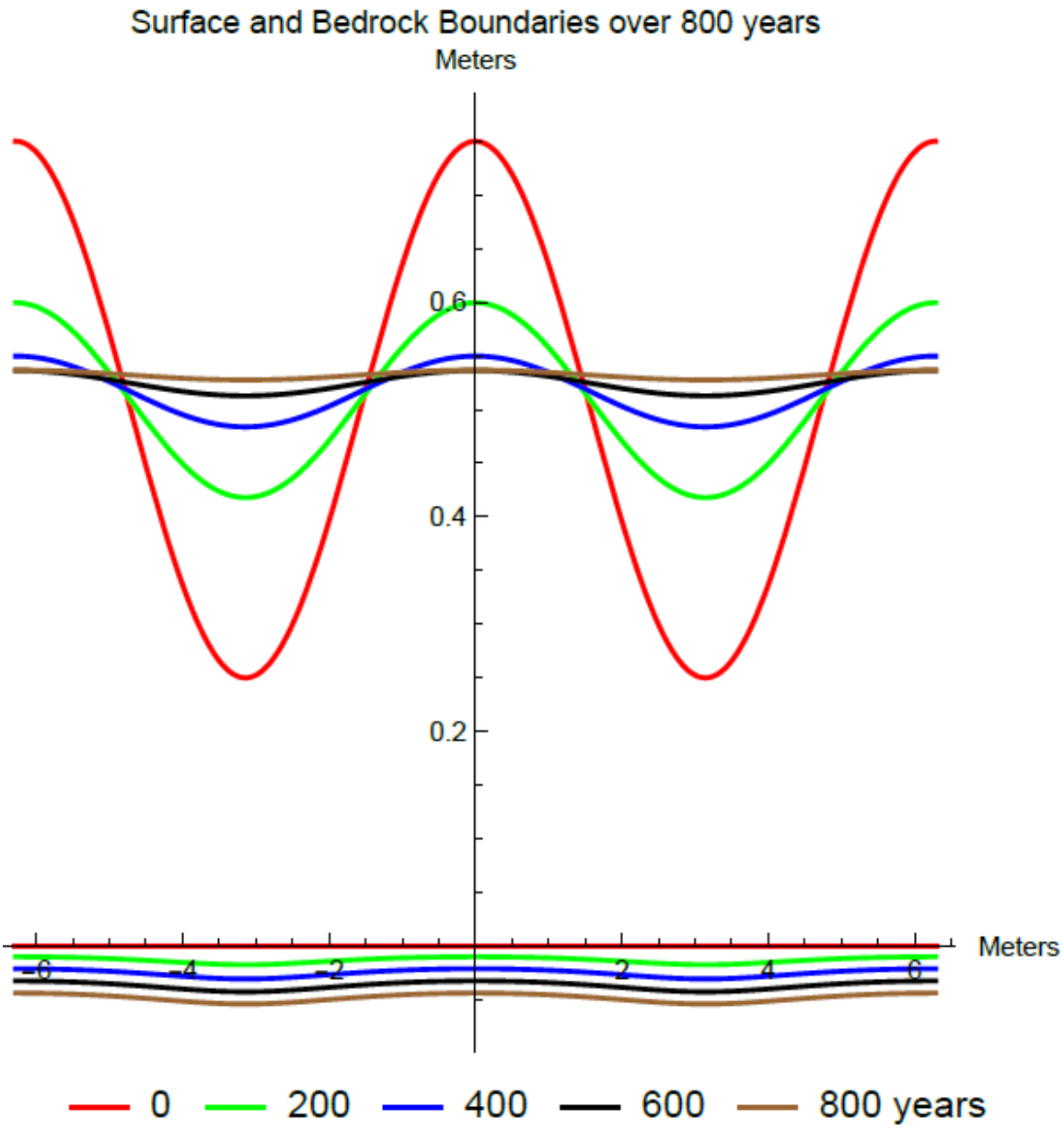

Fig. 7a. Sinusoidal surface and flat bedrock evolution over 800 years. Surface curvature decreases while bedrock curvature reaches a maximum.

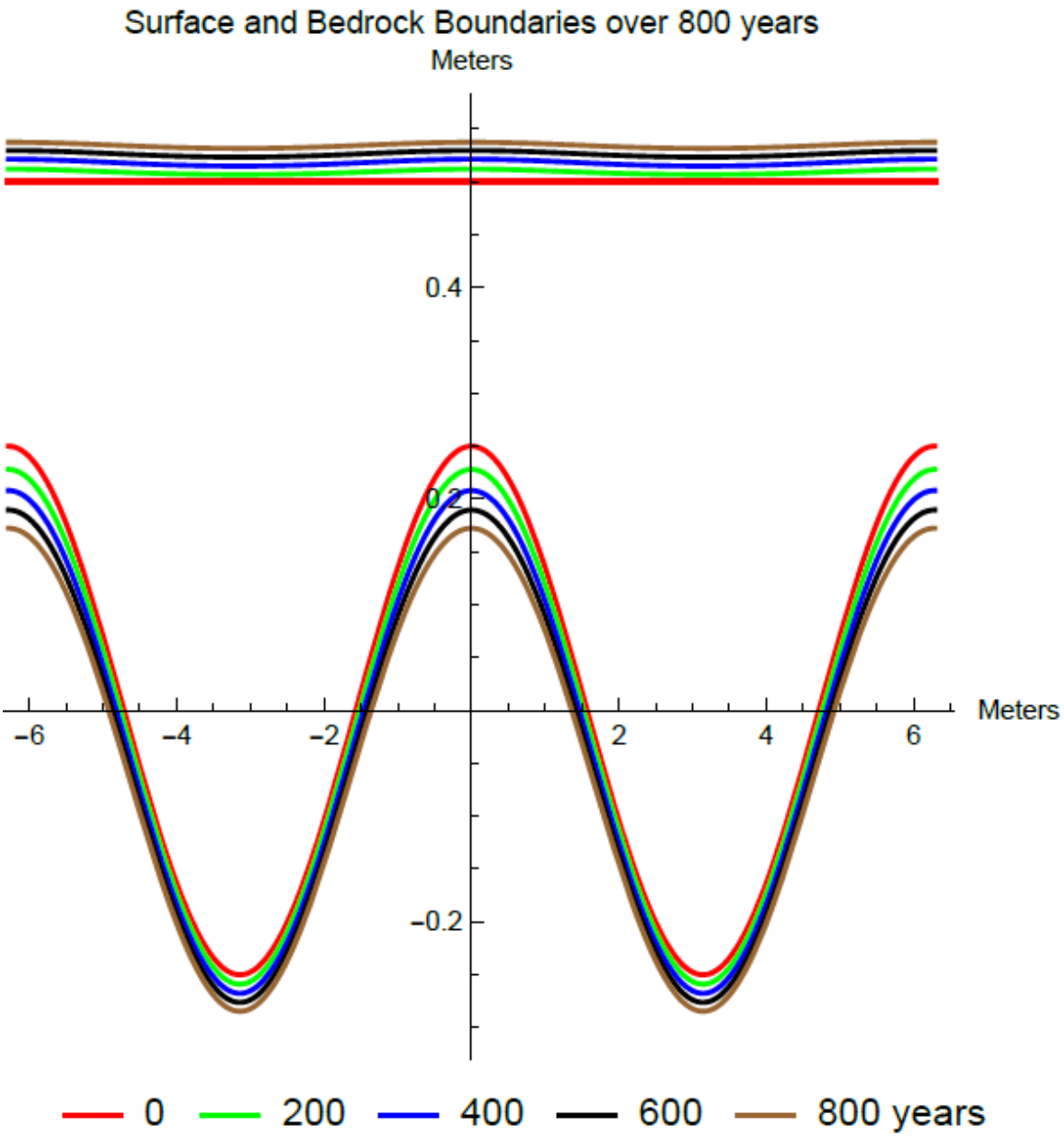

Fig. 7b. Flat surface and sinusoidal bedrock evolution over 800 years. Surface curvature reaches a maximum while bedrock curvature decreases slowly.

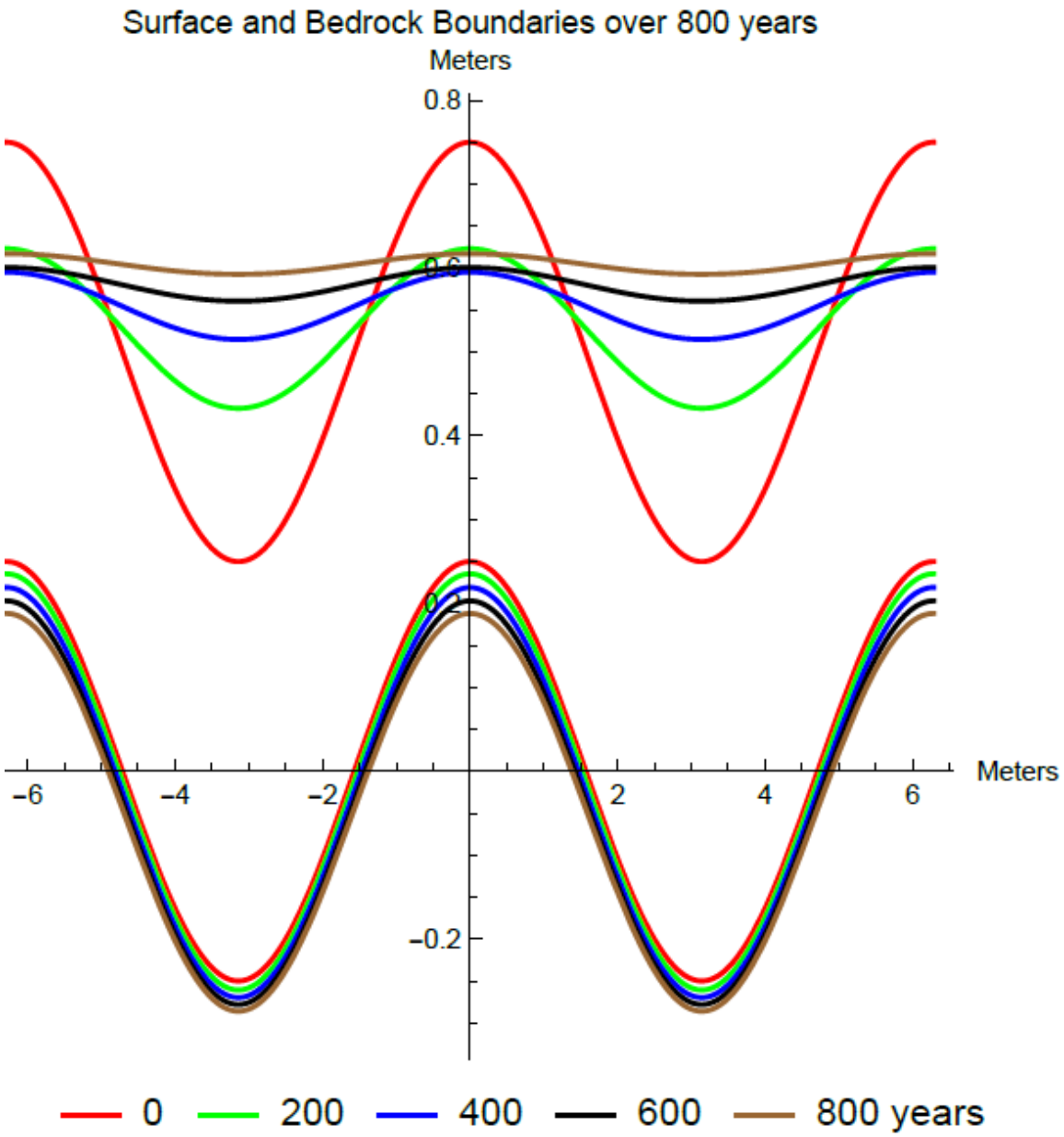

Fig. 7c. Sinusoidal surface and bedrock evolution over 800 years. Both curves exhibit decreased amplitude, but at vastly different rates.

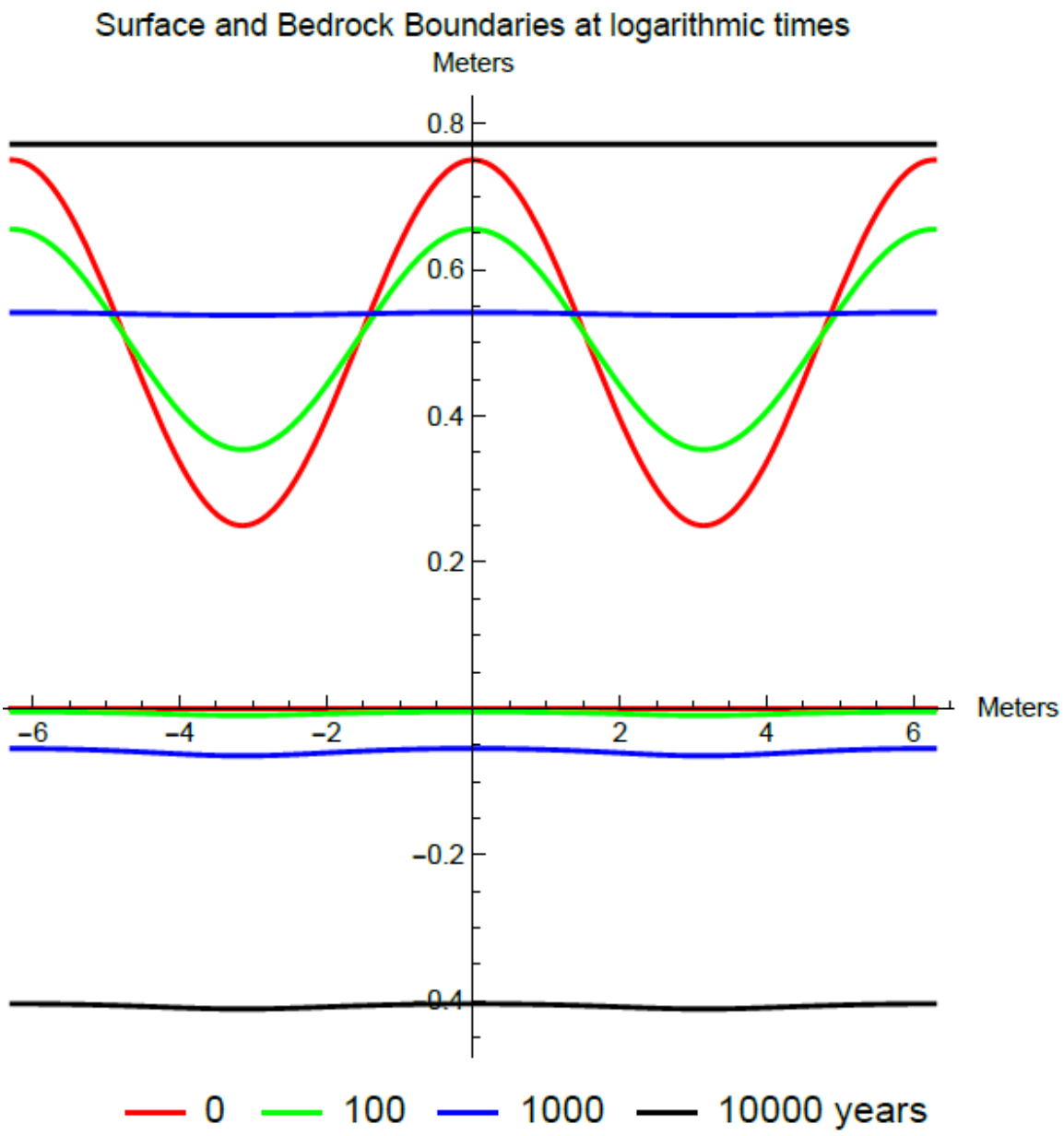

Fig. 8a. Sinusoidal surface and flat bedrock evolution over 10,000 years. Some curvature remains in the bedrock layer as soil accumulates to a flat surface.

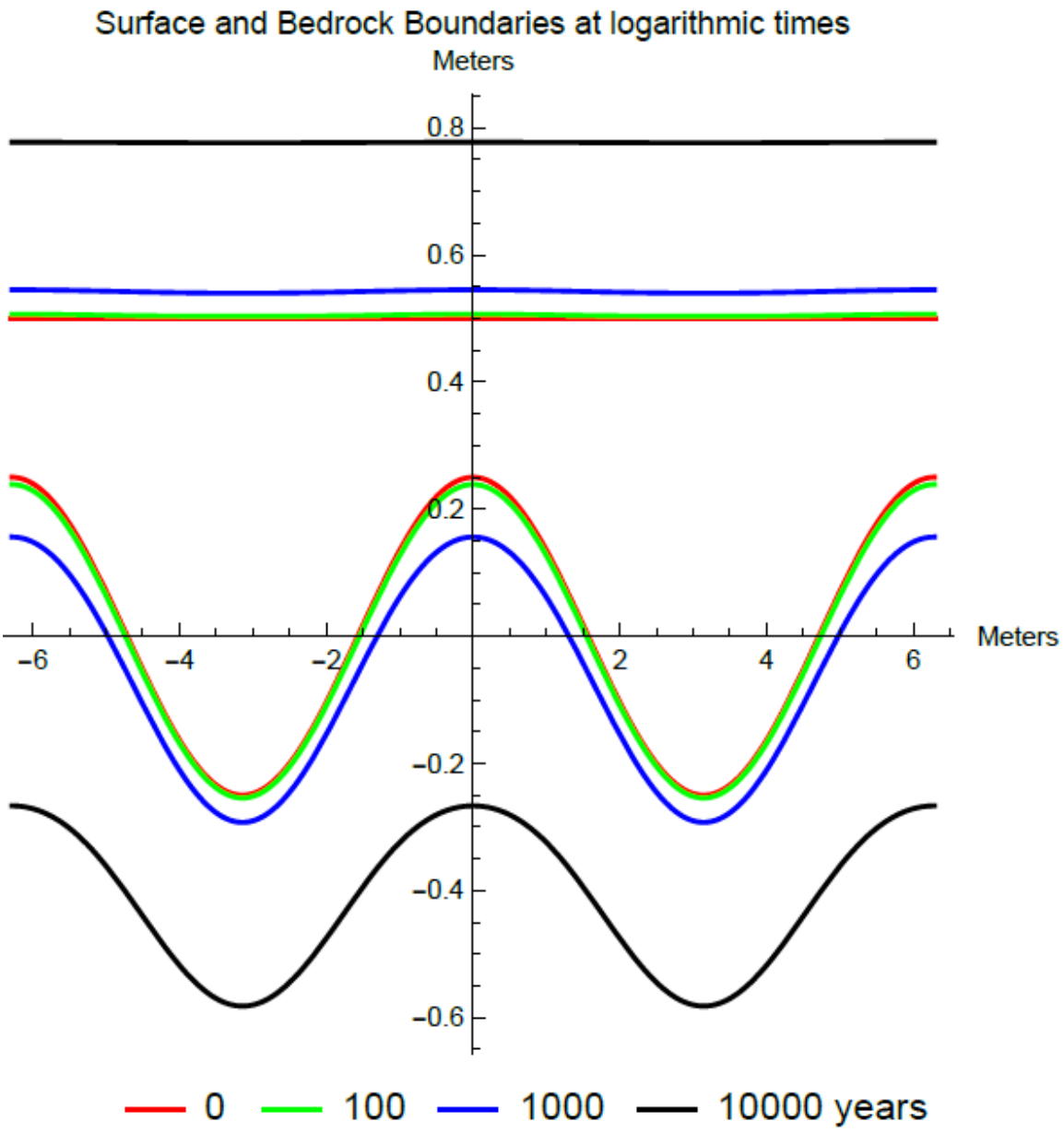

Fig. 8b. Flat surface and sinusoidal bedrock evolution over 10,000 years. Significant curvature remains in the bedrock layer as soil accumulates to a flat surface.

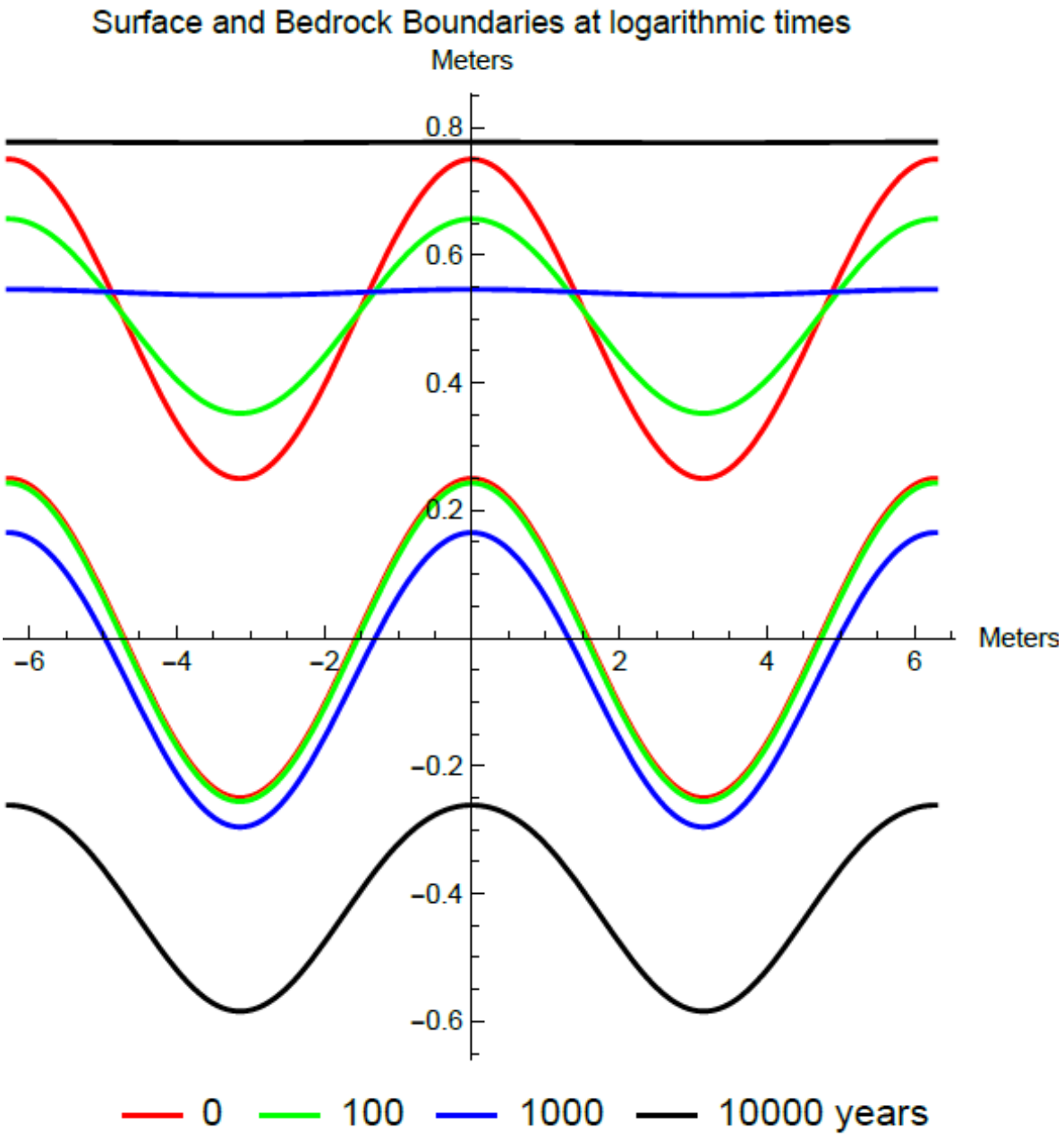

Fig. 8c. Sinusoidal surface and bedrock evolution over 10,000 years. Significant curvature remains in the bedrock layer as soil accumulates to a flat surface.

4.2 Comparison with different models

In this section, evolution of the SvS system based on different theoretical models is presented and compared with the power-law model used in the previous section.

First, the soil production model is compared with and without erosion. As time goes on, the model without erosion shows greater production. This appears to be a consequence of the relative longevity of the shallower depths. Without erosion from the top, it is only the local production variance that evens them out. This is demonstrated in figure 9, without erosion, the decrease in curvature is concentrated in the valleys.

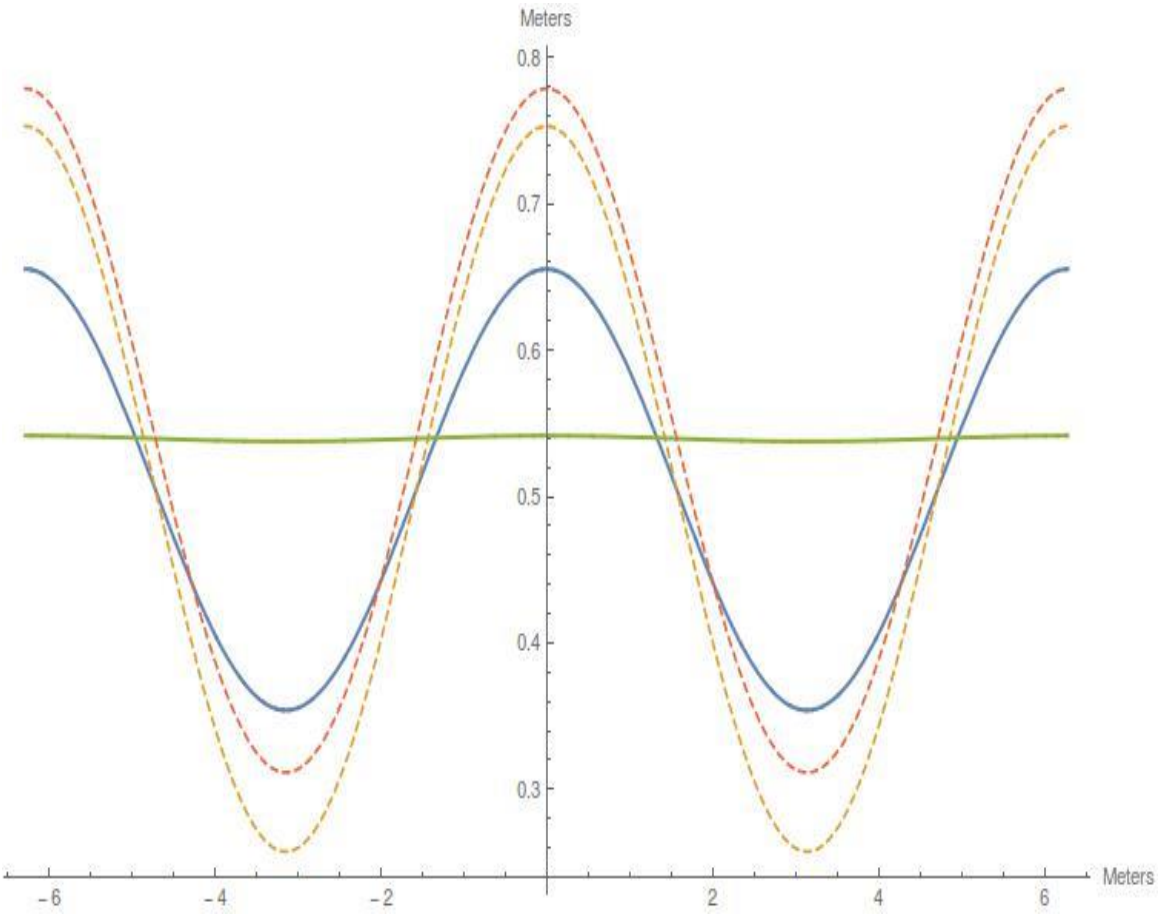

Fig. 9. Surface curvature at 100 and 1000 years. Dashed lines are without erosion.

A competing formulation for soil production by Heimsath [21] replaces the power law term with an inverse exponential source. Some interpretation of their parameters was required for consistency with the formulation of this thesis as they are all fitted to experimental data. Values within the range of data they employed were used and the results were found to match well, with the exponential model being slightly slower. In figure 10 they are compared for the double sinusoid geometry. This choice of initial conditions focuses on the shape of the landscape while avoiding the wildly different scaling of the two functions at extremely small or large soil depths. Despite the lower production, the exponential model appears to have flattened more rapidly.

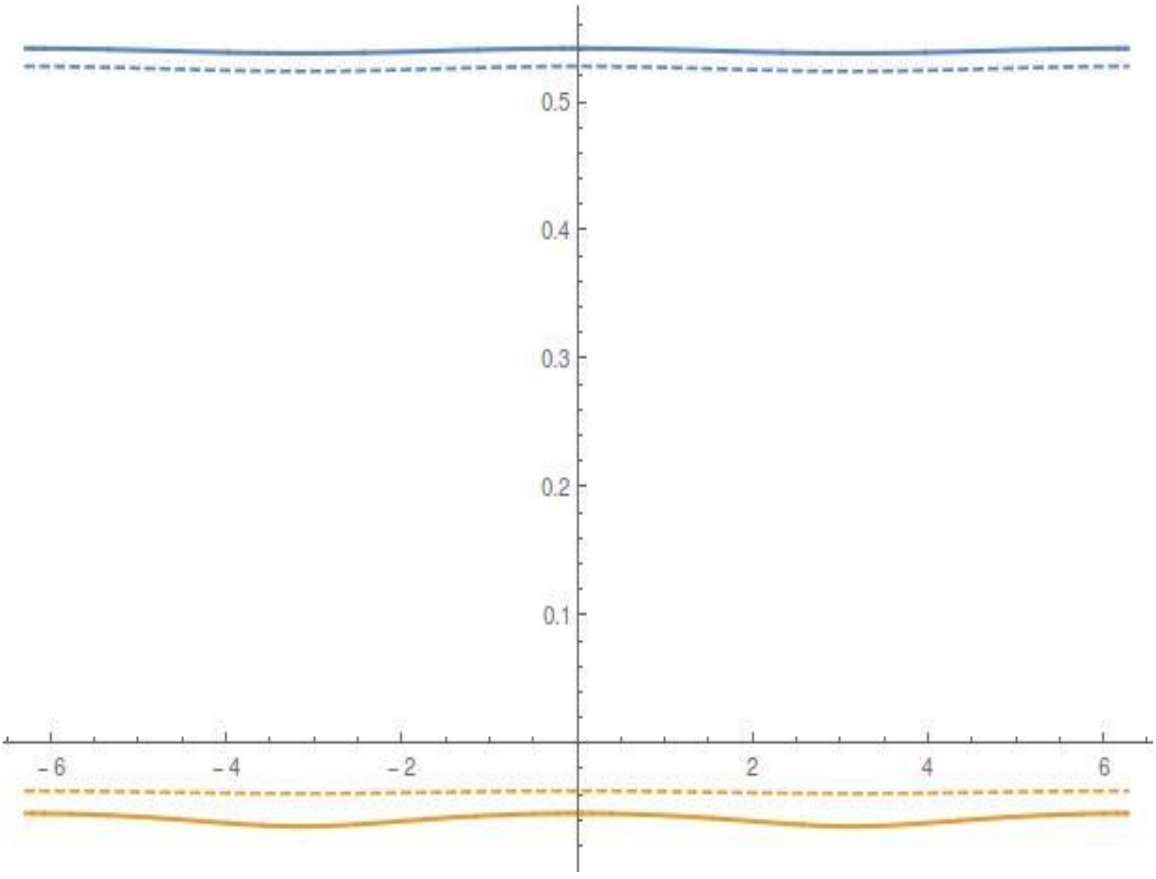

Fig. 10. Surface and bedrock curvature at 1000 yrs. Exponential (dashed) and power law (solid) models.

The work of Kinner and Moody [22] has suggested a curvature dependent erosion. For this comparison, a variance of one third above or below average groundwater infiltration (.2-.4 m/yr rather than a constant .3 m/yr) across the landscape is incorporated proportional to the second spatial derivative. The difference was found to be negligible as shown in Figure 11.

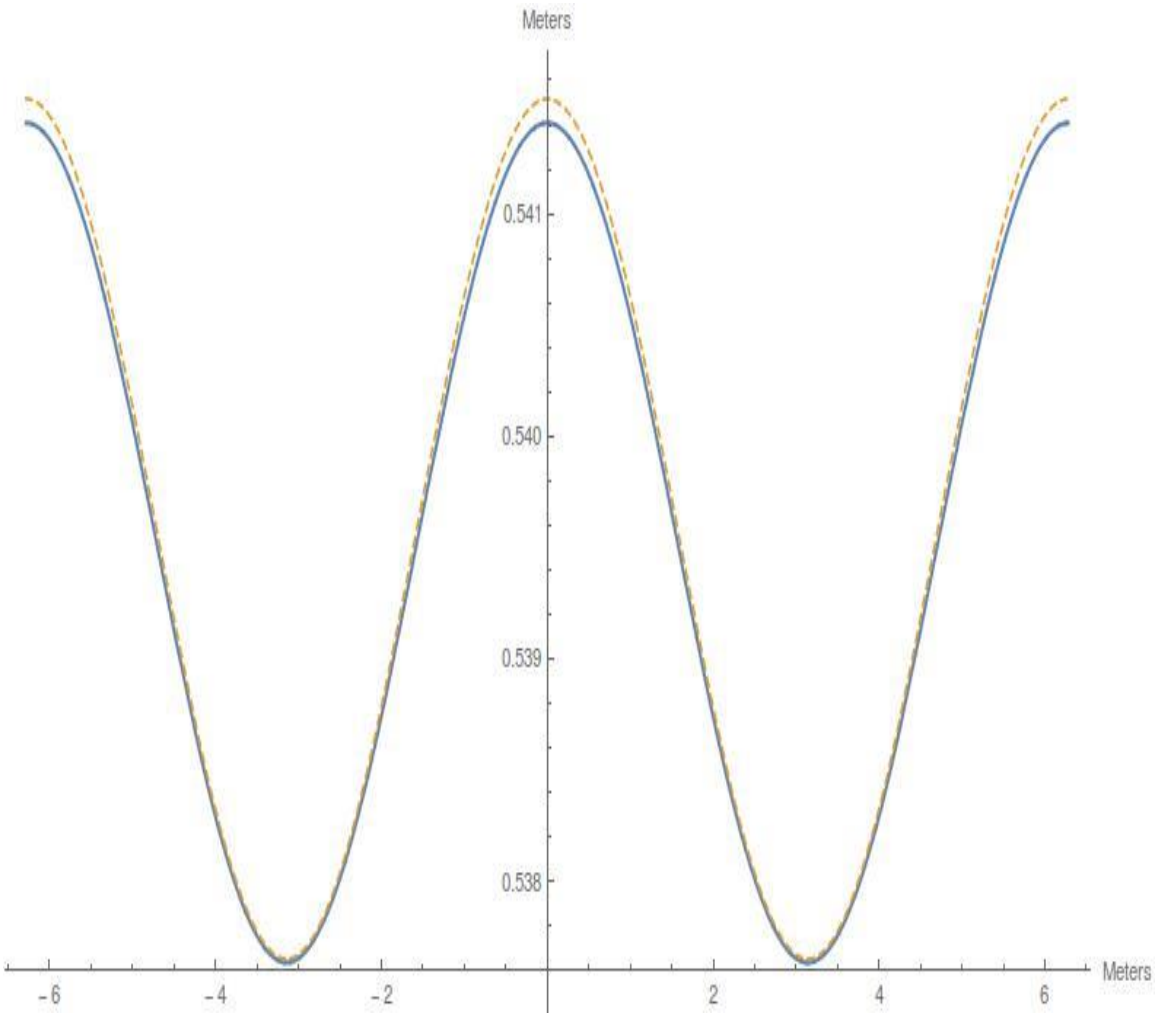

Fig.11. Surface curvature with (dashed) and without (solid) a curvature dependent infiltration rate.

5. Conclusion

5.1 Long-term predictions of soil production/mass flow

Taken together, the comparisons made between different initial conditions and with different formulations suggest that a power-law based model of soil production with surface erosion is most sensitive to conditions in the first few hundred years, varies largely with typical soil depths rather than variations, and fills in valleys more rapidly than it erodes peaks. This last point seem to be due to the overall rise from production across the landscape.

5.2 Further work-analysis

An analysis of the three dimensional results should be conducted. Though there were no obvious features not apparent in two dimensions, the non-linearity of the equations should result in coupling between features along different axes. This may also prompt a rethinking of the quantities used to characterize the results. A method of separating initial conditions into regimes of behavior would be useful. The presence of finite time for feature propagation between layers presently seems the most illustrative property.

5.3 Further Work-Theoretical Improvements

The bond process considered treats locations on the lattice as coordinates and connections between them as abstraction with no physical extent. If formulated as a

site percolation, grain and pores could be treated in the same context. This would necessitate a new theory of transport for grains that may not be diffusive.

The binary separation into mobile soil and stationary bedrock may be inaccurate. While, there is evidence that most of the action occurs along a soil front [23], there must be some finite layer over which the reaction actually occurs. It seems that a treatment of spatially varying conductance would be necessary to address the issue. This also raises questions about whether a process acting on the fractal, accessible cluster is equivalent to one acting uniformly on the medium. The boundaries are also a concern. The relation between surface and volume dimensionalities should be investigated if flow in particular directions is to be determined.

5.3 Further Work-Numerical Improvements

Improvements to the numerical solution might start with a different choice of mesh. Non-periodic boundary conditions possibly could be used with a different mesh as previously mentioned in this documentation [18]. The standard solvers in Mathematica were used, which, while professionally coded, are general purpose. The problem may well benefit from a custom-built program. There are methods of error-approximation for many of these methods and results from these could guide the development of code.

The parameters employed in equations for landscape evolution would preferably be predicted rather than experimental. Values of D in a random environment are given in Hughes [12]. Combining these with some geophysical considerations may be relatively

simple. Barring that, studies of geological samples must provide these values. Most such data do not record values directly useful to this approach and parameters must be inferred. A change in preferred measures on soil samples would be of great benefit. Perhaps the most practical solution would be to conduct controlled laboratory experiments on random media without the noise of natural environments. These complications are, of course, relevant to any practical theory of landscape evolution, but their absence would allow for careful examination of the model's mathematical foundations.

References

1. Burbank, D. W., & Anderson, R. S. (2011). *Tectonic geomorphology*. John Wiley & Sons.

2. Aharony, A., & Stauffer, D. (2003). *Introduction to percolation theory*. Taylor & Francis.

3. Hunt, A., Ewing, R., & Ghanbarian, B. (2014). *Percolation theory for flow in porous media* (Vol. 880). Springer.

4. Molnar, P., & Cronin, T. W. (2015). Growth of the Maritime Continent and its possible contribution to recurring Ice Ages. *Paleoceanography*, *30*(3), 196-225.

5. Gnedenko, B. V., & Kolmogorov, A. N. Limit Distributions for Sums of Independent Random Variables (1954). *Cambridge, Mass*.

6. Reif, F. (2009). *Fundamentals of statistical and thermal physics*. Waveland Press.

7. Hunt, A. G., Skinner, T. E., Ewing, R. P., & Ghanbarian-Alavijeh, B. (2011). Dispersion of solutes in porous media. *The European Physical Journal B-Condensed Matter and Complex Systems*, *80*(4), 411-432.

8. Blöschl, G., & Sivapalan, M. (1995). Scale issues in hydrological modelling: a review. *Hydrological processes*, *9*(3-4), 251-290.

9. Yu F., & Hunt, A. G., (2018). Predicting soil formation on the basis of transport-limited chemical weathering. *Geomorphology*, 301 21-27.

10. Bernabé, Y., & Bruderer, C. (1998). Effect of the variance of pore size distribution on the transport properties of heterogeneous networks. *Journal of Geophysical Research: Solid Earth*, *103*(B1), 513-525.

11. Ghanbarian, B., Hunt, A. G., Ewing, R. P., & Sahimi, M. (2013). Tortuosity in porous media: a critical review. *Soil science society of America journal*, *77*(5), 1461-1477.

12. Hughes, B. D. (1995). Random walks and random environments. *Oxford*, *2*, 1995-1996.

13. Fisher, M. E. (1961). Critical probabilities for cluster size and percolation problems. *Journal of Mathematical Physics*, *2*(4), 620-627.

14. Ambegaokar, V., Halperin, B. I., & Langer, J. S. (1971). Hopping conductivity in disordered systems. *Physical review B*, *4*(8), 2612.

15. Sheppard, A. P., Knackstedt, M. A., Pinczewski, W. V., & Sahimi, M. (1999). Invasion percolation: new algorithms and universality classes. *Journal of Physics A: Mathematical and General*, *32*(49), L521.

16. Lee, Y., Andrade Jr, J. S., Buldyrev, S. V., Dokholyan, N. V., Havlin, S., King, P. R., ... & Stanley, H. E. (1999). Traveling time and traveling length in critical percolation clusters. *Physical Review E*, *60*(3), 3425.

17. Hunt, A. G., & Sahimi, M. (2017). Flow, Transport and Reaction in Porous Media: Percolation Scaling, Critical-Path Analysis, and Effective-Medium Approximation. *Rev. Geophys*

18. https://reference.wolfram.com/language/tutorial/NDSolveMethodOfLines.html#1306392612

19. Hunt, A. G. (2016). Spatio-temporal scaling of vegetation growth and soil formation from percolation theory. *Vadose Zone Journal*, *15*(2).

20. Ahnert, F. (1987). Approaches to dynamic equilibrium in theoretical simulations of slope development. *Earth Surface Processes and Landforms*, *12*(1), 3-15.

21. Heimsath, A. M., Dietrich, W. E., Nishiizumi, K., & Finkel, R. C. (1997). The soil production function and landscape equilibrium. *Nature*, *388*(6640), 358.

22. Kinner, D. A., & Moody, J. A. (2010). Spatial variability of steady-state infiltration into a two-layer soil system on burned hillslopes. *Journal of Hydrology*, *381*(3), 322-332.

23. Dixon, J. L., Heimsath, A. M., & Amundson, R. (2009). The critical role of climate and saprolite weathering in landscape evolution. *Earth Surface Processes and Landforms*, *34*(11), 1507-1521.